Accepted Manuscript

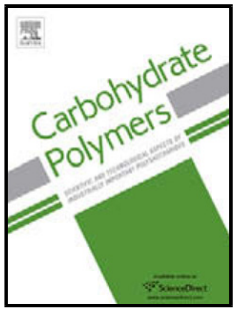

Title: Mineralized agar-based nanocomposite films: Potential food packaging materials with antimicrobial properties

Authors: Ivana Malagurski, Steva Levic, Aleksandra Nesic, Miodrag Mitric, Vladimir Pavlovic, Suzana Dimitrijevic-Brankovic

PII: S0144-8617(17)30840-8
DOI: http://dx.doi.org/doi:10.1016/j.carbpol.2017.07.064
Reference: CARP 12581

To appear in:

Received date: 13-4-2017
Revised date: 18-7-2017
Accepted date: 21-7-2017

Please cite this article as: Malagurski, Ivana., Levic, Steva., Nesic, Aleksandra., Mitric, Miodrag., Pavlovic, Vladimir., & Dimitrijevic-Brankovic, Suzana., Mineralized agar-based nanocomposite films: Potential food packaging materials with antimicrobial properties.*Carbohydrate Polymers* http://dx.doi.org/10.1016/j.carbpol.2017.07.064

Mineralized agar-based nanocomposite films: Potential food packaging materials with antimicrobial properties

Ivana Malagurski[a,*], Steva Levic[b], Aleksandra Nesic[c], Miodrag Mitric[c], Vladimir Pavlovic[b], Suzana Dimitrijevic-Brankovic[a]

[a] *University of Belgrade, Faculty of Technology and Metallurgy, 11000 Belgrade, Serbia*

[b] *University of Belgrade, Faculty of Agriculture, 11081 Belgrade, Serbia*

[c] *University of Belgrade, Vinca Institute of Nuclear Science, Mike Petrovica Alasa 12-14, P.O. Box 522, 11001 Belgrade, Serbia*

Corresponding author: Ivana Malagurski

Tel: +381(0)11 3303788

Fax: +381(0)11 3370387

E-mail: madzovska@tmf.bg.ac.rs

Highlights

- Agar was impregnated with Zn-minerals to produce nanocomposite films
- Nanocomposites exhibited different morphologies, properties and functionality
- Reinforcing with minerals improved mechanical, optical and thermal properties
- Nanocomposite films release Zn(II) inducing antimicrobial effect

Abstract

New mineralized, agar-based nanocomposite films (Zn-carbonate and Zn-phosphate/agar) were produced by a combination of *in situ* precipitation and a casting method. The presence of minerals significantly influenced the morphology, properties and functionality of the obtained nanocomposites. Reinforcement with the Zn-mineral phase improved the mechanical properties of the carbonate-mineralized films, but had a negligible effect on the phosphate-mineralized samples. Both nanocomposites showed improved optical and thermal properties, better Zn(II) release potential in a slightly acidic environment and exhibited antimicrobial activity against *S. aureus*. These results suggest that Zn-mineralized agar nanocomposite films could be potentially used as affordable, eco-friendly and active food packaging materials.

Keywords: Agar; Zinc; Nanocomposites; Food packaging; Antimicrobial activity

1. Introduction

Biopolymer-based materials possess many desirable properties that make them an attractive alternative to petroleum-based materials in the area of food packaging. Development of such packaging materials offers significant economic and environmental advantages because they are biodegradable, biocompatible, edible and isolated from renewable resources like plants or algae (Rhim & Ng, 2007). Additionally, these natural-based materials act, not only as barriers, but also as scaffolds for incorporation of additives in the form of antimicrobial agents, antioxidants and nutrients which enhance their functionality. Although numerous biopolymers like carbohydrates, proteins and lipids have been studied as a base for eco-friendly packaging materials, carbohydrates are regarded as the most suitable for food applications due to their great film-forming and moderate mechanical and barrier properties (Zafar et al., 2016).

One such highly attractive polysaccharide is agar. Agar is a carbohydrate synthesized by red algae of the class *Rhodophyceae.* It is composed of agarose and agaropectin. Agarose is a neutral, linear molecule of β-1,3-linked-D-galactose and α-1,4-linked 3,6-anhydro-L-galactose units and mediates gelling of agar hydrogels, while agaropectin is a charged, sulfated, branched, non-gelling unit (Raphael, Avallaneda, Manzolli, & Pawlicka, 2010). So far, numerous agar-based food packaging materials in the form of films and coatings have been investigated (Atef, Rezaei, & Behrooz, 2014; Wang & Rhim, 2015). However, there are still certain limitations for their application in the food packaging industry. First, agar-based materials usually have poor mechanical properties and low thermal stability which can interfere with material processing and handling during production. Second, they lack functionality in terms of antibacterial activity and exhibit poor optical properties which can greatly affect food quality and shelf-life.

The most widely used method for improvement of agar-based material is to combine them with another component in order to obtain composite materials. By definition, a composite is a material made from at least two different components, with resulting properties significantly better than its constituents alone (Zafar et al., 2016). If one of these components has nanometer dimensions, then it is a nanocomposite. Due to high surface to volume ratio, these nano-sized constituents, or nanofillers, interact with other constituent

more intimately, and by using less material, enhanced nanocomposites in terms of mechanical, thermal and barrier properties can be obtained. According to the literature, many agar-based nanocomposite films have been developed. It has been shown that the incorporation of nanoclay (Rhim, 2011; Rhim, 2012), nanocellulose (Reddy & Rhim, 2014), or metallic nanoparticles (Arfat, Ahmed, & Jacob, 2017; Kanmani & Rhim, 2014b) into agar, has the capacity to significantly improve the obtained nanocomposites properties. Also, if these nanofillers contain metals with strong antimicrobial effect, like zinc (Lemire, Harrison, & Turner, 2013), the resulting nanocomposite transforms into an active package with microbicidal activity.

The simplest approach for nanocomposites production is to add a nanofiller to an agar solution prior to film formation, however sometimes, a reinforcing agent can be introduced into agar matrix by *in situ* synthesis. This approach was successful in the case of agar/hydroxyapatite (Hu et al., 2016) and agar/gelatin/hydroxyapatite (Deng, Wang, Zhang, Li, & Wei, 2013) nanocomposites for biomedical applications where hydroxyapatite was formed within agar hydrogel by mineralization through electrophoretic deposition or an immersion technique. A similar strategy could be employed for production of mineral-impregnated agar films. Additionally, if the reinforcing minerals are zinc salts, the resulting nanocomposite could be improved both in a structural and functional sense.

The main objective of this study was to develop a concept of new Zn-mineralized-agar nanocomposite films as potential improved and active food packaging materials and to investigate the effect of reinforcement with Zn-minerals on the obtained nanocomposite properties (morphology, thermal stability, mechanical and optical properties) and functionality (antimicrobial activity against *Escherichia coli, Staphylococcus aureus* and *Candida albicans*).

2. Materials and methods

2.1. Materials

Agar, Nutrient Broth and Agar (NB and NA), Malt Extract Broth and Agar (MEB and MEA) were obtained from HiMedia Laboratories (India). Disodium carbonate, disodium hydrogen phosphate and zinc nitrate hexahydrate were purchased from Sigma Aldrich (USA). Polyglycerol (PG) in the form of a mixture of 85 % diglycerol, triglycerol and

tetraglycerol with trace amounts of glycerol, was supplied by Solvay (Belgium). Release kinetics media, ethanol and acetic acid, were purchased from Zorka Pharma (Serbia).

2.2. Preparation of mineralized agar-based films

Mineralized agar-based nanocomposite films were synthesized by a combination of *in situ* mineral phase formation within agar and a solvent casting method. Film solutions were prepared by dissolving agar in distilled water, under constant stirring, at 100 ^{o}C until boiling. Before addition of the other film components, the temperature of agar solution was decreased to 60 ^{o}C. Then, polyglycerol, as a plasticizer, $Zn(NO_3)_2$ and different mineral precursors (Na_2CO_3 or Na_2HPO_4) were added to the film solution, while mixing constantly at 60 ^{o}C for 45 min. The formation of a Zn-mineral phase within agar solution was immediately visible. 15 g of each formulation of the obtained film solution was poured into a Petri dish, leveled to ensure uniform thickness, and then dried at 37 ^{o}C for 48 h (**Fig. 1**).

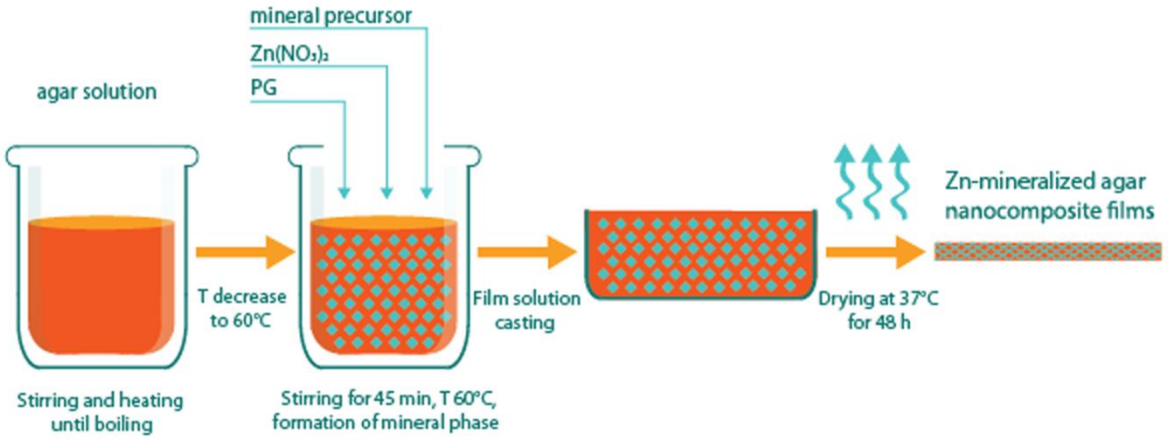

Figure 1. Schematic representation of mineralized-agar nanocomposites preparation procedure.

Non-mineralized, control agar films were produced as described above, except no Zn(II) or mineral precursors were added to the film solution.

Free Zn-mineral precipitates were made by mixing saturated solutions of $Zn(NO_3)_2$ and Na_2CO_3 or Na_2HPO_4. The obtained free Zn-minerals were extensively washed with distilled water, filtered and dried at 37 ^{o}C until reaching constant mass.

Sample codes and corresponding formulations are presented in **Table 1**.

2.3. Characterization

2.3.1. Scanning electron microscopy (SEM)

Surface morphology of the obtained nanocomposites was examined using a JEOL JSM-6390LV SEM (JEOL). Before examination, the samples were coated with gold using a Bal-Tec SCD 005 sputter coater.

Elemental analysis of the gold coated sample surface was investigated using energy-dispersive X-ray spectroscopy **(**EDX) analysis (Oxford Instruments).

2.3.2. X-ray diffraction (XRD)

XRD patterns were acquired on a Philips PW 1050 diffractometer with a Cu-$K\alpha_{1,2}$ radiation source (Ni filter) at room temperature. Measurements were collected in 2θ range of 10 - 60°, scanning step width of 0.05° and 4 s $step^{-1}$. The X-ray line-profile fitting program (XFIT) with a Fundamental parameters convolution approach to generating line profiles (Cheary & Coelho, 1992) was used for the calculation of crystallite size.

2.3.3. Fourier-transformed infrared spectroscopy (FTIR)

FTIR analysis was performed using a FTIR spectrometer IRAffinity-1 (SHIMADZU) in the spectral range 4000 – 500 cm^{-1}, and resolution of 4 cm^{-1}. Prior to analysis, the samples were mixed with KBr, pulverized and compressed into pellets.

2.3.4. Mechanical characterization

An Instron M 1185 universal testing machine was used to obtain the stress-strain curves for the tensile tests of the films. Crosshead speed was 2 mm min^{-1} for all testing samples. From these curves, Young modulus (E, MPa), tensile strength (TS, MPa) and elongation at break (ε, %) of the films were determined. Prior to testing, the films were conditioned in an environmental chamber at 25 ^{o}C and 50 % relative humidity for 24 h. The measurements were done at room temperature and six samples (mold 4.92 x 26.73 x 0.06 mm) for each formulation were tested. The obtained values of the Young's modulus, stress and the elongation at break were within ± 5 %.

2.3.5. Optical properties

Optical properties of the obtained films in the ultraviolet and visible spectral range were determined using a UV-VIS spectrophotometer HALO DB-20S (Dynamica Scientific Ltd. Switzerland). Films were cut into strips 10 x 40 mm and placed in a spectrophotometer test

cell perpendicularly to the light beam. Film transparency (*T*) was calculated using the following equation (1) (Han & Floros, 1997):

$$T = A/x \quad (1)$$

where *A* is the absorbance of films measured at 600 nm, and *x* is the film thickness in mm.

2.3.6. Thermogravimetric analysis (TGA)

TGA was performed on a SDT 2960 TGA/DSC Analyzer (TA INSTRUMENTS). The data were collected under following conditions: dynamic air atmosphere (flow rate 20 ml min^{-1}), 30 – 1000 ^{o}C temperature range and heating rate of 20 ^{o}C min^{-1}.

2.3.7. Total Zn(II) content and Zn(II) release potential

The quantity of Zn(II) in Zn-mineralized agar composites was determined using inductively coupled plasma mass spectrometry (ICP-MS). An accurately weighed amount of film was digested with hydrogen peroxide (30 % w/w) and nitric acid (70 % w/w), in a microwave oven. Upon cooling, appropriate dilutions were made using distilled water and the zinc concentration was measured. Total Zn(II) content of the samples was expressed as mg of Zn per g of the film material.

Zn(II) release potential of the nanocomposites was studied in static conditions at room temperature (25 ^{o}C), using 2 different media: 10 % ethanol and 3 % acetic acid as liquid food simulants (Plastics Europe, 2011). The samples were cut into 30 x 10 mm strips and placed into flasks with 10 ml of medium. At the end of incubation period (day 7), medium was taken and concentration of released Zn(II) was measured by ICP-MS.

2.4. Antimicrobial activity

Antimicrobial potential of the Zn-mineralized agar films was evaluated against Gram-negative bacteria *Escherichia coli* (ATCC 25922), Gram-positive bacteria *Staphylococcus aureus* (ATCC 25923) and fungus *Candida albicans* (ATCC 10231). The antimicrobial assay was conducted using a modified Broth macrodilution method in suspension cultures. Prior to investigation, the films were UV sterilized. Aliquots of overnight microorganism cultures were added to the wells with samples and medium (NB and MEB for bacteria and fungus, respectively), providing the initial concentration of $\sim 10^5$ CFU ml^{-1} for microorganisms and 50 mg ml^{-1} for the samples. After 24 h of incubation, serial dilutions of media samples were plated on NA and MEA, for bacteria and fungus, respectively. The number of colony forming

units was determined after incubation for 24 h at 37 ºC. The antimicrobial activity of tested samples was established by decrease in $\log_{10}$ CFU ml^{-1} of the test culture during incubation. Positive controls were prepared according to the same procedure, except no sample was added to the suspension cultures.

2.5. Statistical analysis

Statistical analysis was done using Student's t-test and one-way ANOVA plus Tukey's test. The results are presented as mean ± standard deviations (SD). Each experimental point was performed in triplicate. The values were considered to be statistically different at $p \leq 0.05$.

3. Results and discussion

3.1. Morphology of Zn-mineralized agar nanocomposite films

Zn-mineralized agar nanocomposite films were successfully produced by a combination of *in situ* mineral phase deposition and solvent casting method. SEM micrographs of the control and the nanocomposites film surfaces are shown in **Fig. 2a-c.**

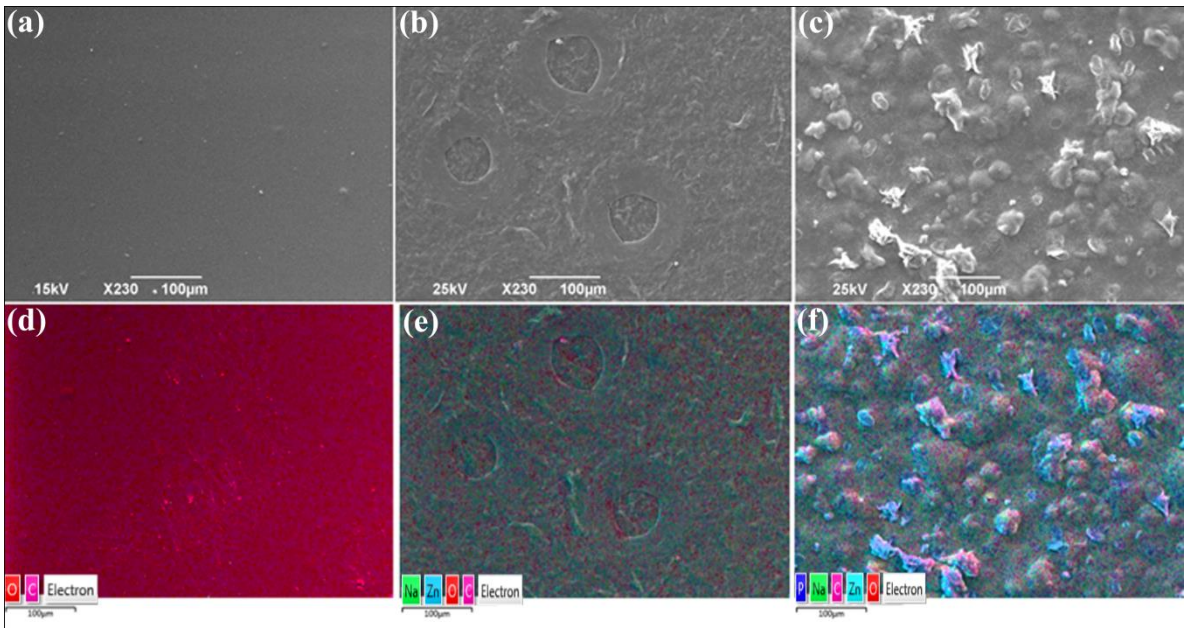

Figure 2. Morphology of control agar film and Zn-mineralized agar composites: SEM micrographs of: (a) A; (b) AC and (c) AP. EDX analysis of: (d) A; (e) AC and (f) AP.

As it can be seen in **Fig. 2a-c**, SEM micrographs of the samples showed a significant difference between the control (**Fig. 2a**) and the nanocomposites (**Fig. 2b** and **2c**). Control films appeared smooth and homogenous, while the incorporated, mineral phase was clearly

visible in the nanocomposites. There was also a difference in surface morphology between nanocomposite samples: the carbonate mineral within the AC sample was apparently smaller in size and more uniformly distributed throughout the agar matrix (**Fig. 2b**), in contrast to the AP sample, where phosphate phase was in the form of agglomerates randomly distributed into agar matrix (**Fig. 2c**). In addition, EDX analysis confirmed different elemental composition of samples with different formulations (**Fig. 2d-f**).

3.2. XRD analysis

Mineral identification and polymorphy were investigated using XRD analysis. XRD patterns of the obtained nanocomposites, control films and free minerals are shown in **Fig. 3a** and **3b.**

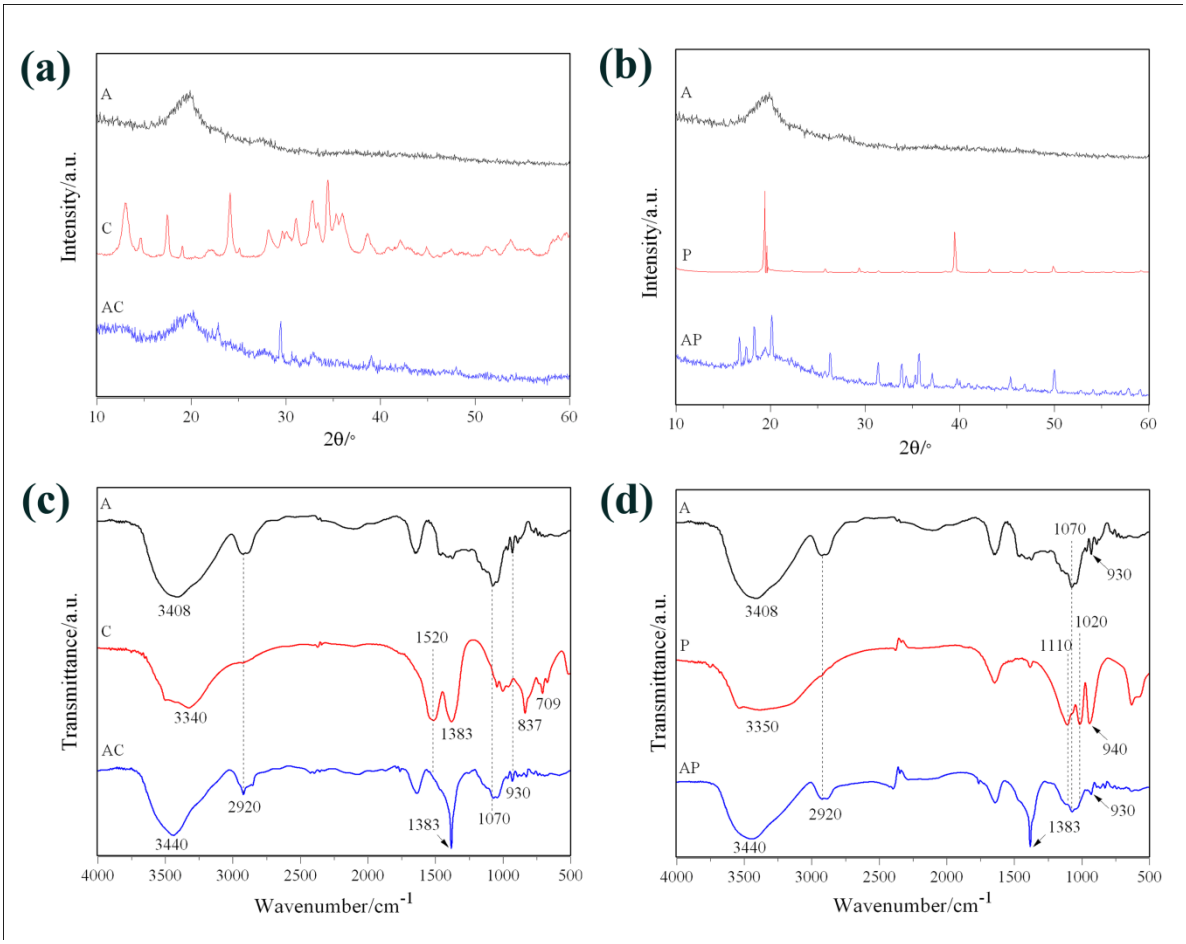

Figure 3. Sample characterization: XRD patterns of: (a) AC and (b) AP; FTIR spectra of: (c) AC and (d) AP.

In our previous work free mineral phases were identified as $Zn_5(CO_3)_2(OH)_6$ with a relatively small amount of $ZnCO_3$ and $Zn_4(CO_3)(OH)_6$ for carbonate, and $Zn_3(PO_4)_2(H_2O)_4$

for phosphates, with corresponding crystallites sizes of ~ 22 and ~ 43 nm, respectively (Malagurski et al., 2017). As it can be seen in **Fig. 3a** and **3b**, the control sample (A) showed diffuse diffraction patterns, characteristic for agar (Arfat et al., 2017; Freile-Pelegrin et al., 2007) which have significantly changed after incorporation of the mineral phase.

For the AC sample, it was found that carbonate mineral phase was composed of poorly defined $Zn_5(CO_3)_2(OH)_6$, with significant presence of $NaNO_3$ and, most probably, NaOH (**Fig. 3a**). The crystallite size in sample AC was ~ 4 nm, which is in good agreement with results reported by Malagurski et al. (2017) for formation of a Zn-carbonate phase in the presence of alginate.

In the case of the AP sample, the mineral phase formed within agar was identified as $Zn_3(PO_4)_2(H_2O)_4$, with crystallite size around 45 nm.

It can be concluded that only the formation of carbonate mineral phase was significantly affected by the presence of agar, which resulted in an almost 5.5 times reduction of crystallite size when compared to free carbonate minerals, while phosphate minerals preserved their morphology and size in both environments. According to Oaki and Imai (2003), the formation of various crystals in the presence of agar is primarily affected by gel density. In dense gels the diffusion is limited and thus affected crystal growth more, changing crystals morphology towards more irregular polycrystalline aggregates. However, in this study, the formation of mineral phases occurred primarily in agar film solution (*i.e.* it is similar to conventional precipitation method), therefore potential limitations for mineral precursors diffusion or crystallite growth were avoided.

Although the presence of agar did not influence the formation of both Zn-minerals in the same manner, incorporation of both mineral phases within agar matrix resulted in the formation of stable and compact nanocomposite films.

3.3. FTIR analysis

The FTIR spectra of the nanocomposites, control films and free minerals are presented in **Fig. 3c** and **3d**. FTIR analysis was used to confirm the presence of a mineral phase within agar and to detect potential interactions between components of the obtained nanocomposites.

The FTIR spectrum of the neat agar film (see **Fig. S1** in Supplementary) was quite typical for agar with bands at 3447 cm^{-1} (OH- stretching vibrations), ~ 2930 cm^{-1} (C-H vibrations),

1070 cm^{-1} (C-O-C vibrations) and 931 cm^{-1} (C-O vibrations) (Kanmani & Rhim, 2014a; Yang et al., 2014). The addition of polyglycerol (sample A, **Fig. 3c**) caused an increase in the intensity of bands in the spectral region 2950 - 2850 cm^{-1}. Also, the position of the band related to the OH- stretching vibrations was shifted to a lower position (*i.e.* 3408 cm^{-1}) which suggested the formation of new interactions (*e.g.* hydrogen bonding) inside the agar matrix.

Free zinc carbonate and free zinc phosphate minerals exhibited the bands that are in agreement with literature data for these minerals (Jung et al., 2009; Malagurski et al., 2017). The FTIR spectra of the mineralized agar films was very similar to that of control. However, the shift in the position of OH- bands (3400-3450 cm^{-1}) might suggest the formation of hydrogen bonds between the mineral phase and the polymer matrix (Xie et al., 2010). Also, the new band at 1383 cm^{-1} could represent a residual nitrate anion (from $Zn(NO_3)_2$) that remained after synthesis (Singh & Rath, 2015).

3.4. Film thickness and mechanical characterization

The wide range of applicability of any film as a packaging material is significantly pertained to its mechanical properties such as tensile strength and elongation at break. The tensile strength of the obtained samples is presented in **Table 2**.

It can be seen that the incorporation of the Zn-mineral phase within agar influenced both thickness and mechanical properties of the obtained samples. The thickness of the control agar film was 60 μm and it increased to 70 – 90 μm after incorporation of the Zn-mineral phase. This is expected because film thickness depends on the solid content. There was no difference in thickness between nanocomposite films with different formulations. As for the mechanical characterization, the presence of the carbonates significantly increased the TS value of the AC nanocomposite when compared to the control films: 20.52 and 0.39 MPa, respectively. Also, the Young's modulus values for the AC and AP samples were higher than the corresponding value of the control agar films. However, when agar matrix was impregnated with the phosphates (sample AP), the change in the TS value when compared to control agar film was negligible (**Table 2**).

An increase in TS usually implies a decrease in elongation at break of the material, and the same trend was observed in our study. Incorporation of the mineral phase within agar

matrix resulted in a decrease of the ε values for both nanocomposite formulations, when compared to the control, this effect was more pronounced for the AC sample (**Table 2**).

The obtained results are in good agreement with literature data. The improvement of mechanical properties of biopolymer-based films upon reinforcing with nanofillers is quite common and it has been reported for agar-based nanocomposites impregnated with nanoclay (Jang et al., 2010), nanoparticles (Arfat et al., 2017; Kanmani et al., 2014b) or biomolecules (Atef et al., 2014; Reddy et al., 2014). However, in situations when a nanofiller is present in excess (Orsuwan, Shankar, Wang, Sothomvit, & Rhim, 2016; Rhim, 2011) or when constituents of the nanocomposite are not biocompatible (Gimenez, Lopez de Lacey, Perez-Santín, Lopez-Caballero, & Montero, 2013), even a decline in the overall nanocomposite physical properties can be observed.

Mechanical properties of nanocomposites are highly affected by interactions between its constituents. If there are strong interfacial interactions between the nano-phase and the polymer matrix (*e.g.* extensive hydrogen bonding), they will result in multiple inter- and intra-polymer chain associations and, subsequently, improved mechanical properties (Alexandre & Dubois, 2000). This was the case with the AC nanocomposite, where, being smaller in size, the carbonate crystallites were uniformly distributed throughout the agar matrix and mediated more intimate interactions with polymer molecules. In contrast to that, the phosphate crystallites were larger in size and exhibited a tendency to agglomerate causing phase-separation and heterogeneous appearance of the AP sample which led to a negligible change in the TS. The obtained results are supported by SEM evaluation (Section 3.1.) and XRD analysis (Section 3.2.) where it was shown that agar was actively involved in the carbonate phase formation.

Elongation at break, as a measure of film elasticity, was decreased in both nanocomposite films. This can be explained by the fact that intermolecular interactions between both mineral phases and matrix molecules were strong enough to decrease free volume between polymer chains and restrict their movement at the mineral-agar interface (Wang et al., 2005).

According to the conventional standards, the tensile strength of packaging material needs to be higher than 3.5 MPa (Kim, Lee, & Park, 1995). Thus, the AC film presented in this work satisfies this criteria and can potentially be applicable in the food packaging industry.

3.5. Optical properties

The optical properties of food packaging materials are important in prevention of photodegradation of food products during storage time. Hence, the transmission rate of ultraviolet (100-400 nm) and visible light (400-700 nm) trough food packaging material has important role in designing the right package that can preserve and protect the food products. Macroscopic images of the control and the nanocomposite films are shown in **Fig. 4a-c.**

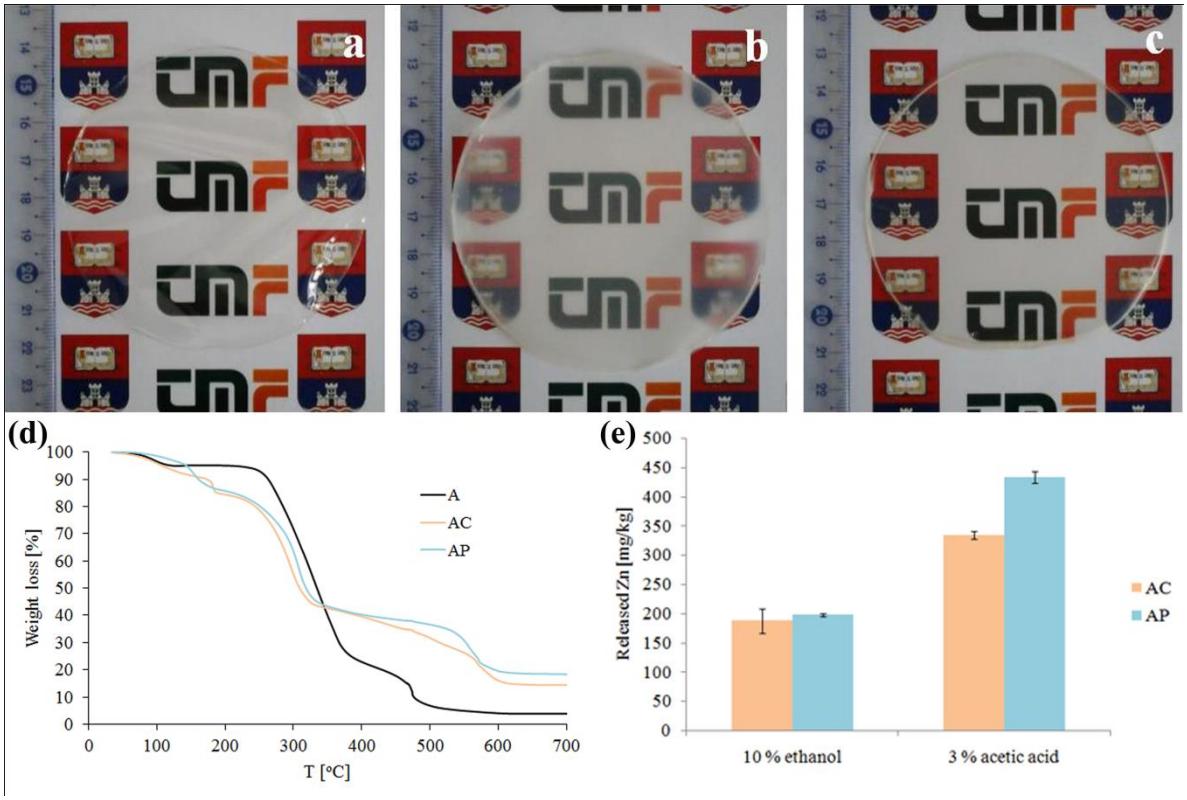

Figure 4. Sample characterization: Film transparency: (a) A; (b) AC and (c) AP. TGA results: (d) control agar and nanocomposite films with different formulations. Release kinetics: (e) cumulative Zn(II) release from mineralized samples, after 7 days of incubation in 10 % ethanol and 3 % acetic acid.

It can be seen that film transparency decreased with the formation of the mineral phase, as follows: A > AP > AC. Although, the films with mineral phases visually exhibited lower transparency compared to the control film, all films were still visually transparent and clear, which is a desirable property for packaging materials, because they should enable visual observation of packed products. Evaluation of light transmission (%) at selected wavelengths indicated that the presence of mineral phase within agar has significantly decreased transmittance of the obtained nanocomposites, especially in the UV region (**Table 3**). Also, the AC samples were more effective than the AP in UV blockage due to uniform and

homogenous dispersion of Zn-carbonate within polymer (**Fig. 1e**) The obtained results are in agreement with macroscopic-visual observations of the nanocomposite films.

Polysaccharide-based films are usually transparent and require addition of materials that can block light transmission. Light barrier properties can be improved by addition of various materials such as essential oils (Hosseini, Rezaei, Zandi, & Farahmandghavi, 2015) or nanoparticles into a film structure (Arfat et al., 2017). The obtained results indicate that Zn-mineralized films can effectively block light, which is important property of active packaging, especially in the case of sensitive food.

3.7. TG analysis

The TG analysis curves of control and nanocomposites are presented in **Fig. 4d.**

TG analysis of the control film indicated two phases of mass loss: up to temperatures of 170 ^{o}C, initial mass loss due to dehydratation; followed by thermal degradation of agar and polyglycerol ($T \geq 200$ ^{o}C) (Orsuwan et al., 2016; Shankar, Teng, & Rhim, 2014). It can be seen (**Fig. 4d)** that the presence of Zn-mineral phase has modified the thermal degradation properties of the obtained samples. Both nanocomposites exhibited similar degradation patterns up to a certain temperature: initial weight loss due to dehydratation ($T \leq 170$ ^{o}C), followed by organic phase degradation ($200 \leq T \leq 370$ ^{o}C). From this stage, thermal degradation curves varied depending on the type of the mineral phase and also exhibited different profiles when compared to the control sample. In both nanocomposites, agar continued to decompose, but at lower rates. Also Zn-carbonate from the AC nanocomposite, started decomposing to ZnO and CO_2 contributing to the overall weight loss ($400 \leq T \leq 600$ ^{o}C), while the phosphate incorporated in the AP sample, remained stable explaining the highest residual mass after thermal decomposition.

When comparing initial stages of weight loss due to water desorption, a difference in water content among control and nanocomposite can be observed. Water, as the major hydrogel constituent, can be found in three different forms: 1) free water; 2) intermediate water which weakly interacts with both mineral phase and polymer network and is nor bound nor free; and 3) bound water which strongly interacts with both components of the nanocomposite, and has a different aggregation state than free water (Jhon & Andrade, 1973). During air drying at 37 ^{o}C, only free water is being evaporated. From the obtained results, it

can be concluded that the incorporation of mineral phase into agar has increased the total amount of intermediate and bound water due to increase in number of charged groups that can interact with water molecules. As for the starting point of agar degradation, it can be seen in **Fig. 4d** that the presence of mineral phase did not change it. However, in T region above 340 ^{o}C, nanocomposites exhibited different thermal degradation profiles when compared to the control, indicating that the presence of mineral phase has thermally stabilized the nanocomposites.

3.8. Zn(II) content and release kinetics

Total Zn(II) content of the obtained nanocomposites, expressed as mg of Zn per g of the film material, was determined using ICP-MS. Results are presented in **Table 2.**

Release kinetics were evaluated to illustrate Zn(II) migration to food in potential applications as food packaging materials. Cumulative Zn(II) release profiles from the nanocomposites, expressed as mg of released Zn per kg of release medium, are presented in **Fig. 4e**. It can be observed that both nanocomposites released a similar amount of Zn in 10 % ethanol, however when placed in 3 % acetic acid, the total Zn release was quite improved, and the phosphate-mineralized films showed greater Zn-release potential than the carbonate ones. Taking into account that Zn-minerals are insoluble in water and ethanol, only the fraction of Zn(II) sorbed on the polymer chains was released in 10 % ethanol, explaining the similar result for both nanocomposites. In addition, the lower pH values of acetic acid supports the Zn-mineral phase dissolution, contributing to the overall Zn release, with phosphates being more soluble than carbonates under tested conditions.

The results presented in this work showed that Zn release from the nanocomposite films could be modulated by changing the nanocomposite formulation, thus providing the opportunity for optimization towards specific applications.

3.9. Antimicrobial activity

Results of the antimicrobial evaluation are presented in **Table 4**.

It can be seen that the control films did not exhibit antimicrobial activity, as expected, and the tested microorganisms showed different sensitivities towards the antimicrobial potential of the nanocomposites. Treatment of *S. aureus* and *C. albicans* with both nanocomposite

formulations, resulted in an antimicrobial effect, with complete biocidal action for *S. aureus* after 24 h. On the other hand, *E. coli* was only mildly inhibited. In addition, both AC and AP samples exhibited similar antimicrobial potential.

The antimicrobial effect of the Zn-mineralized samples was additionally confirmed using a disc diffusion method (data shown in the Supplementary file, **Fig. S2**).

Antimicrobial activity of the obtained nanocomposites is mediated through the released Zn(II) from the incorporated Zn-mineral phase (Kasemets, Ivask, Dubourguier, & Kahru, 2009). Zn is a transitional metal with strong antimicrobial activity and the mechanisms of its biocidal action are based either on inactivation of evolutionary conserved enzymes involved in essential metabolic pathways (*e.g.* energy production or biomolecule synthesis) or antioxidants depletion (Lemire et al., 2013). The observation that Zn-mineralized nanocomposites were apparently more effective in elimination of Gram-positive bacteria is in agreement with literature data and can be explained by differences in bacterial cell wall structure between Gram-positive and Gram-negative bacteria (Soderberg, Agren, Tengruo, Hallmans, & Banck, 1989). Similar findings were reported for nanocomposites impregnated with ZnO nanoparticles (Anitha, Brabu, John-Thiruvadigal, Gopalakrishnan, & Natarajan, 2012, Kanmani et al., 2014b; Marra, Silvestre, Duraccio, & Cimmino, 2016).

4. Conclusion

In this study, new agar-based nanocomposites reinforced with Zn-minerals (Zn-carbonate or Zn-phosphate) were successfully synthesized by a combination of *in situ* precipitation and a casting method. The presence of the mineral phase within the agar matrix was confirmed by SEM, EDX, FTIR and XRD analysis. Incorporation of Zn-minerals into agar significantly affected nanocomposite films morphology, properties and functionality. Carbonate minerals were smaller in size and uniformly dispersed through the agar matrix, which led to the formation of the nanocomposite with improved mechanical properties. Impregnation with phosphates, which exhibited a tendency to agglomerate, had a negligible effect on the corresponding nanocomposite mechanical properties. Both nanocomposites have shown improved optical and thermal properties, better release potential in a slightly acidic environment and strong antimicrobial action against *S. aureus*. Enhanced mechanical and light barrier properties combined with functionality in terms of antimicrobial activity,

facilitate processing and handling procedures associated with packaging materials, which could potentially improve packed food quality and extend shelf-life. The obtained results suggest that Zn-mineralized agar nanocomposite films could potentially be used as affordable, eco-friendly, biodegradable and antimicrobial food packaging materials.

Acknowledgements

This work was supported by the Ministry of Education, Science and Technological Development of the Republic of Serbia [Grant III 45019 and Grant TR31035].

References

Alexandre, M., & Dubois, P. (2000). Polymer-layered silicate nanocomposites: preparation, properties and use of new class of materials. *Material Science and Engineering: R: Reports, 28,* 1-63.

Anitha, S., Brabu, B., John Thiruvadigal, D. Gopalakrishnan, C., Natarajan, T. S. (2012). Optical, bactericidal and water repellent properties of electrospun nano-composite membranes of cellulose acetate and ZnO. *Carbohydrate Polymers, 87,* 1065-1072.

Arfat, Y. A., Ahmed, J., & Jacob, H. (2017). Preparation and characterization of agar-based nanocomposite films reinforced with bimetallic (Ag-Cu) alloy nanoparticles. *Carbohydrate Polymers, 155,* 382-390.

Atef, M., Rezaei. M., & Behrooz, R. (2014). Preparation and characterization agar-based nanocomposite film reinforced by nanocrystalline cellulose. *International Journal of Biological Macromolecules, 70,* 537-544.

Cheary, R. W., & Coelho, A. (1992). A fundamental parameters approach to X-ray line-profile fitting. *Journal of Applied Crystallography, 25,* 109-121.

Deng, Y., Wang, H., Zhang, L., Li, Y., & Wei, S. (2013). *In situ* synthesis and *in vitro* biocompatibility of needle-like nano-hydroxyapatite in agar–gelatin co-hydrogel. *Materials Letters, 104,* 8-12.

Freile-Pelegrín, Y., Madera-Santana, T., Robledo, D., Veleva, L., Quintana, P., & Azamar, J. A. (2007). Degradation of agar films in a humid tropical climate: Thermal, mechanical, morphological and structural changes. *Polymer Degradation and Stability, 92,* 244-252.

Gimenez, B., Lopez de Lacey, A., Perez-Santín, E., Lopez-Caballero, M. E., & Montero, P. (2013). Release of active compounds from agar and agar-gelatin films with green tea extract. *Food Hydrocolloids, 30,* 264-271.

Han, J. H., & Floros, J. D. (1997). Casting antimicrobial packaging films and measuring their physical properties and antimicrobial activity. *Journal of Plastic Film & Sheeting, 13,* 287-298.

Hosseini, S. F., Rezaei, M., Zandi, M., & Farahmandghavi, F. (2015). Bio-based composite edible films containing *Origanum vulgare* L. essential oil. *Industrial Crops and Products, 67,* 403-413.

Hu, J., Zhu, Y., Tong, H., Shen, X., Chen, L., & Ran, J. (2016). A detailed study of homogeneous agarose/hydroxyapatite nanocomposites for load-bearing bone tissue. *International Journal of Biological Macromolecules, 82,* 134-143.

Jhon, M. S., & Andrade, J. D. (1973). Water and hydrogels. *Journal of Biomedical Materials Research: Part A,* 7, 509-522.

Jung, S. H., Oh, E., Shim, D., Park, D. H., Cho, S., Lee, B. R., Jeong, Y. U., Lee, K. H., & Jeong, S. H. (2009). Sonochemical synthesis of amorphous zinc phosphate nanospheres. *Bulletin of the Korean Chemical Society, 30,* 2280-2282.

Kanmani, P., & Rhim, J. W. (2014a). Antimicrobial and physical-mechanical properties of agar-based films incorporated with grapefruit seed extract. *Carbohydrate Polymers, 102,* 708-716.

Kanmani, P., & Rhim, J. W. (2014b). Properties and characterization of bionanocomposite films prepared with various biopolymers and ZnO nanoparticles. *Carbohydrate Polymers, 106,* 190-199.

Kasemets, K., Ivask, A., Dubourguier, H. C., & Kahru, A. (2009). Toxicity of nanoparticles of ZnO, CuO and TiO_2 to yeast *Saccharomyces cerevisiae*. *Toxicology in vitro, 6,* 1116-1122.

Kim, Y. J., Lee, H. M., & Park, O. O. (1995). Processabilities and mechanical properties of Surlyn-treated starch/LDPE blends. *Polymer Engineering & Science, 35,* 1652-1657.

Lemire, J. A., Harrison, J. J., & Turner, R. J. (2013). Antimicrobial activity of metals: mechanisms, molecular targets and applications. *Nature Reviews Microbiology, 11,* 371-384.

Malagurski, I., Levic, S., Pantic, M., Matijasevic, D., Mitric, M., Pavlovic, V., & Dimitrijevic-Brankovic, S. (2017). Synthesis and antimicrobial properties of Zn-mineralized alginate nanocomposites. *Carbohydrate Polymers, 165,* 313-321.

Marra, A., Silvestre, C., Duraccio, D., & Cimmino, S. (2016). Polylactic/zinc oxide biocomposite films for food packaging. *International Journal of Biological Macromolecules, 88,* 254-262.

Oaki, Y., & Imai, H. (2003). Experimental demonstration for the morphological evolution of crystals grown in gel media. *Crystal Growth & Design, 3,* 711-716.

Orsuwan, A., Shankar, S., Wang, L. F., Sothornvit, R., & Rhim, J. W. (2016). Preparation of antimicrobial agar/banana powder blend films reinforced with silver nanoparticles. *Food Hydrocolloids, 60,* 476-485.

Plastics Europe, Explanatory views on Regulation (EU) No. 10/2011 on plastic materials and articles intended to come into contact with food. Available at: http://www.plasticseurope.org/documents/document/20111208094327-foodcontact_pim_explanatory_document_7_december_2011.pdf Accessed on March 30th, 2017.

Raphael, E., Avellaneda, C. O., Manzolli, B., & Pawlicka, A. (2010). Agar-based films for application as polymer electrolytes. *Electrochimica Acta, 55,* 1455-59.

Reddy, J. P., & Rhim, J. W. (2014). Characterization of bionanocomposite films prepared with agar and paper-mulberry pulp nanocellulose. *Carbohydrate Polymers, 110,* 480-488.

Rhim, J. W. (2011). Effect of clay contents on mechanical and water vapor barrier properties of agar-based nanocomposite films. *Carbohydrate Polymers, 86,* 691-699.

Rhim, J. W. (2012). Physical-mechanical properties of agar/k-carrageenan blend film and derived clay nanocomposite film. *Journal of Food Science, 77,* N66-73.

Rhim, R. W., & Ng, P. K. W. (2007). Natural biopolymer-based nanocomposite films for packaging applications. *Critical Reviews in Food Science and Nutrition, 47,* 411-433.

Shankar, S., Teng, X,, & Rhim, J. W. (2014). Properties and characterization of agar/CuNP bionanocomposite films prepared with different copper salts and reducing agents. *Carbohydrate Polymers, 114*, 484-492.

Singh, P. V., & Rath, C. (2015). Passivation of native defects of ZnO by doping Mg detected through various spectroscopic techniques. *RSC Advances, 5*, 44390-97.

Soderberg, T., Agren, M., Tengrup, I., Hallmans, G., & Banck, G. (1989). The effects of an occlusive zinc medicated dressing on the bacterial flora in excised wounds in the rat. *Infection, 17*, 81-85.

Wang, L. F., & Rhim, J. W. (2015). Preparation and application of agar/alginate/collagen ternary blend functional food packaging films. *International Journal of Biological Macromolecules, 80*, 460-468.

Wang, S., Song, C., Chen, G., Gu, T., Liu, J., Zhang, B., & Takeuchi, S. (2005). Characteristics and biodegradation properties of poly(3-hydroxybutyrate-*co*-3-hydroxyvalerate)/organophilic montmorillonite (PHBV/OMMT) nanocomposite. *Polymer Degradation and Stability, 87,* 69-76.

Xie, M., Olderøy, M., Andreassen, J. P., Selbach, S. M., Strand, B. L., & Sikorski, P. (2010). Alginate-controlled formation of nanoscale calcium carbonate and hydroxyapatite mineral phase within hydrogel networks. *Acta Biomaterialia*, *6*, 3665–3675.

Yang, H., Gao, P. F., Wu, W. B., Yang, X. X., Zeng, Q. L., Li, C., & Huang, C. Z. (2014). Antibacterials loaded electrospun composite nanofibers: release profile and sustained antibacterial efficacy. *Polymer Chemistry, 5*, 1965-1975.

Zafar, R., Zia, K. M., Tabasum, S., Jabeen, F., Noreen, A., & Zuber, M. (2016). Polysaccharide based bionanocomposites, properties and applications: A review. *International Journal of Biological Macromolecules, 92*, 1012-1024.

Figure Caption

Figr-1

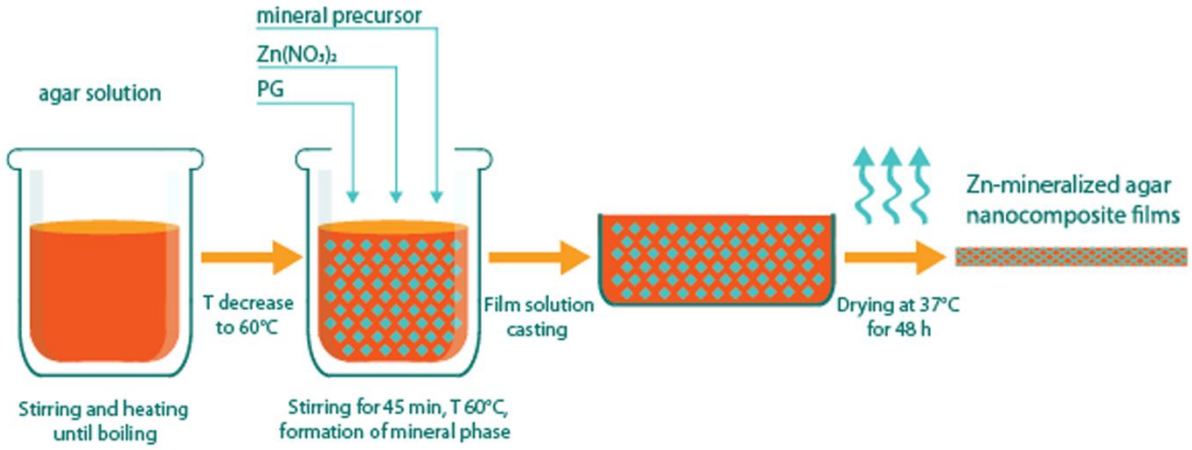

Figr-2

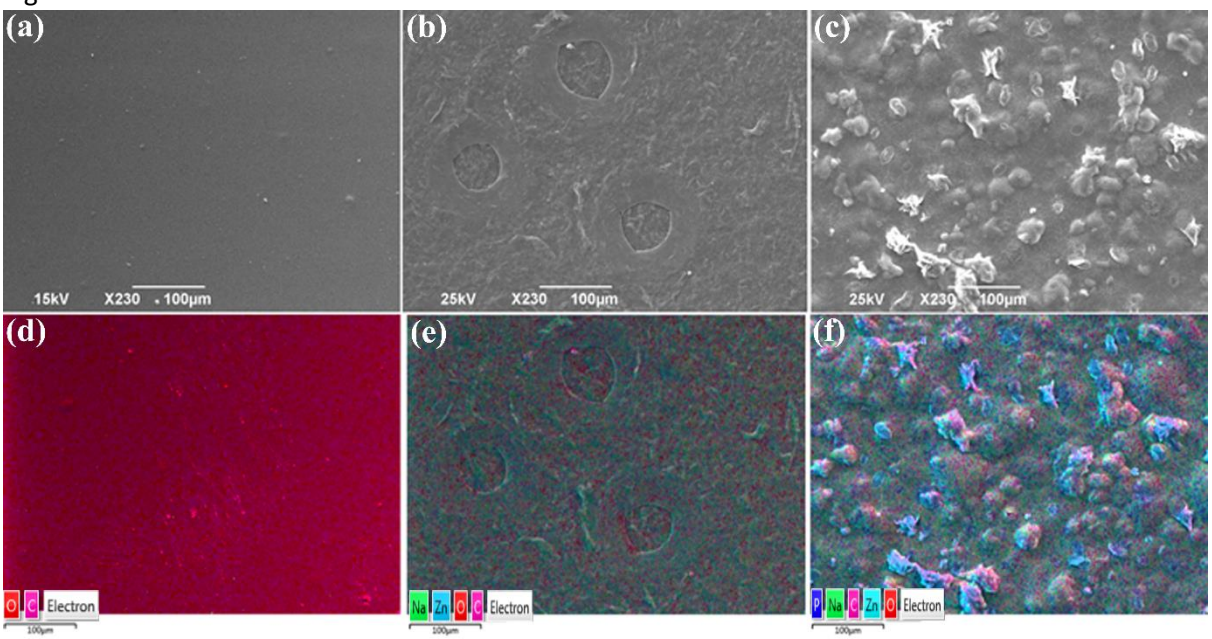

Figr-3

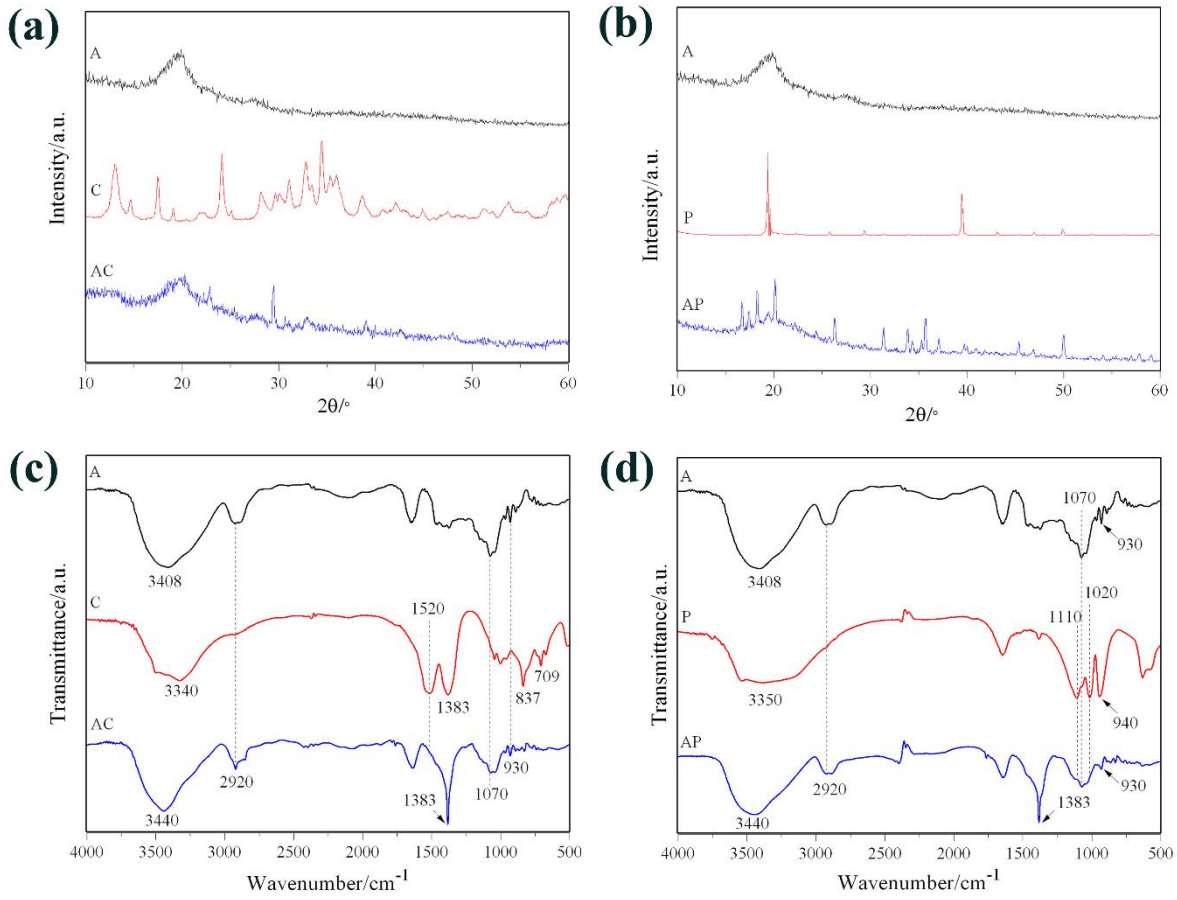

Figr-4

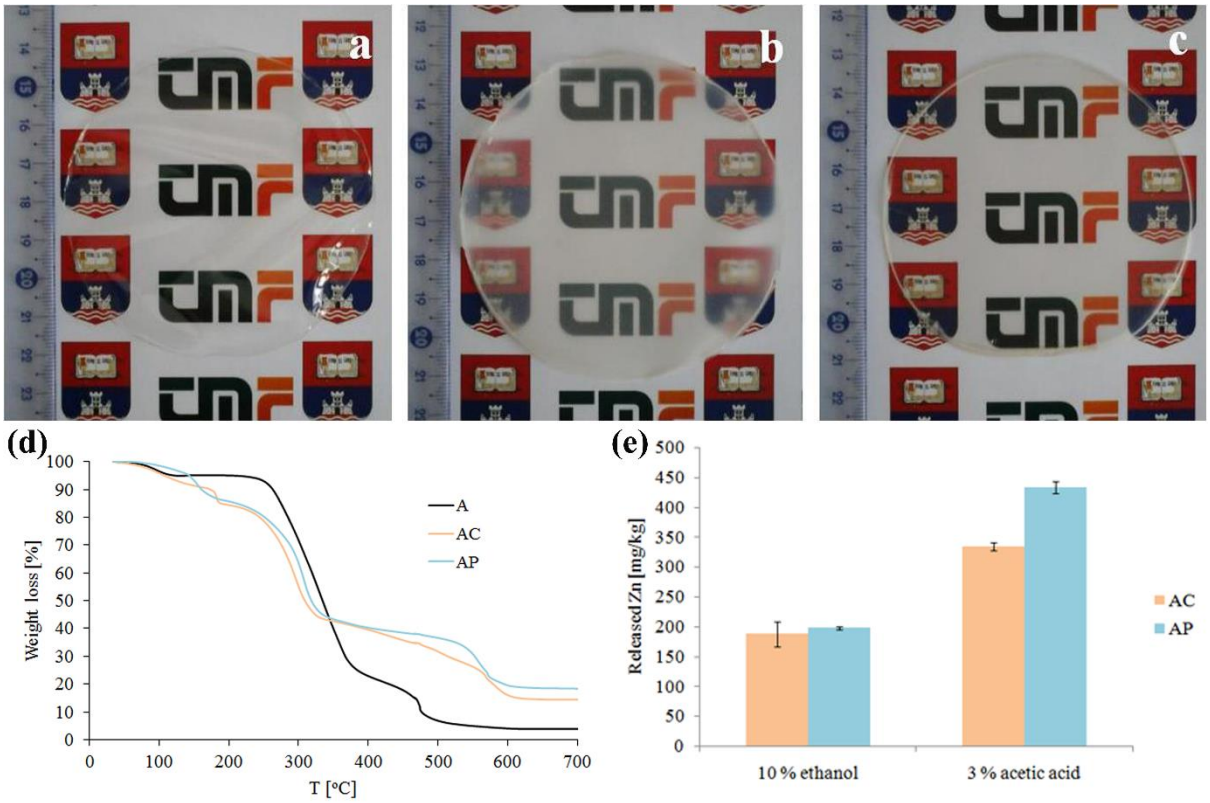

Table 1. Review of sample codes and corresponding formulations.

Sample	Agar [%]	$Zn(NO_3)_2$ [mM]	Mineral precursor		PG [%]
			Na_2CO_3 [mM]	Na_2HPO_4 [mM]	
A[a]	2	-	-	-	
AC[b]	2	50	25	-	30 % w_t/w_t agar
AP[c]	2	50		25	
C[d]	-	100	100	-	-
P[e]	-	100	-	100	-

[a] A, control agar films
[b] AC, agar films mineralized with zinc carbonate
[c] AP, agar films mineralized with zinc phosphate
[d] C, free zinc carbonate minerals
[e] P, free zinc phosphate minerals

Table 2. Summary of sample group thickness, metallic and mineral phase content and mechanical properties.

Sample	Thickness [µm]	Zn(II) content [mg/g]	TS [MPa]	ε [%]	E [MPa]

A	60	/	0.39	18.3	278.5
AP	70 - 90	159 ± 2	1.7	16.3	312.8
AC	70 - 90	194 ± 28	20.52	4.64	3355.7

Table 3. Light transmission and transparency of control and Zn-mineralized nanocomposite films.

Sample	Light transmission at different wavelengths (%)							Transparency
	200 nm	280 nm	350 nm	400 nm	500 nm	600 nm	800 nm	
A	11.1	72.22	84.35	86.74	88.65	89.54	89.7	0.78 ± 0.04
AC	1.77	2.87	8.2	4.16	4.32	5.51	8.3	22.25 ± 4.1
AP	1.76	4.49	13.02	9.72	10.58	12.02	14.51	15.18 ± 0.83

Table 4. Antibacterial activity of control and nanocomposite films against *S. aureus*, *E. coli* and *C. albicans*, expressed as log10 CFU ml^{-1}. MBC - microbicidal activity - growth of the microorganism was not detected.

Microbial strain		**0h**	**24h**
S. aureus	**Control**	**4.9±0.1**	**8.5 ± 0.4[a]**
	+ A		8.7 ± 0.1
	+ AC		MBC
	+ AP		MBC
E. coli	**Control**	**4.9±0.1**	**9.5 ± 0.7**
	+ A		9.1 ± 0.3
	+ AC		6.2 ± 0.3*
	+ AP		6.5 ± 0.2*
C. albicans	**Control**	**5.2±0.1**	**8.2 ± 0.1**
	+ A		7.9 ± 0.4
	+ AC		2.5 ± 0.4*
	+ AP		2.7 ± 0.7*

[a] Significant differences compared to control samples are indicated by asterisk (*$p \leq 0.05$).